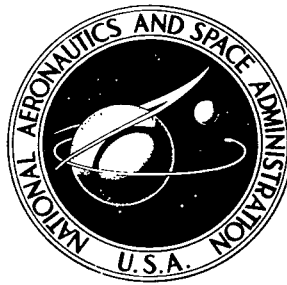


NASA TECHNICAL NOTE



NASA TN D-6127

c.1

NASA TN D-6127



LOAN COPY: RETURN
AFWL (DOGL)
KIRTLAND AFB, N

APPROXIMATE TREATMENT OF V/STOL WALL INTERFERENCE FOR CLOSED CIRCULAR TUNNELS

by Harry H. Heyson
Langley Research Center
Hampton, Va. 23365

NATIONAL AERONAUTICS AND SPACE ADMINISTRATION • WASHINGTON, D. C. • FEBRUARY 1971



0133012

1. Report No. NASA TN D-6127	2. Government Accession No.	3. Recipient's Catalog No.	
4. Title and Subtitle APPROXIMATE TREATMENT OF V/STOL WALL INTERFERENCE FOR CLOSED CIRCULAR TUNNELS		5. Report Date February 1971	
		6. Performing Organization Code	
7. Author(s) Harry H. Heyson		8. Performing Organization Report No. L-7449	
		10. Work Unit No. 721-01-12-01	
9. Performing Organization Name and Address NASA Langley Research Center Hampton, Va. 23365		11. Contract or Grant No.	
		13. Type of Report and Period Covered Technical Note	
12. Sponsoring Agency Name and Address National Aeronautics and Space Administration Washington, D.C. 20546		14. Sponsoring Agency Code	
		15. Supplementary Notes	
16. Abstract An approximate treatment of V/STOL wall interference in a circular tunnel indicates that the interference factors at the model for this tunnel should be of the same order of magnitude as those presently available for a square tunnel of equal cross-sectional area. There is a greater degree of uncertainty with respect to the lateral and longitudinal distributions of interference; however, the available results for the square tunnel should be reasonably close to those of the circular tunnel provided that the model is relatively small in comparison with the test section.			
17. Key Words (Suggested by Author(s)) Wall interference V/STOL Closed circular tunnels		18. Distribution Statement Unclassified - Unlimited	
19. Security Classif. (of this report) Unclassified	20. Security Classif. (of this page) Unclassified	21. No. of Pages 32	22. Price* \$3.00

APPROXIMATE TREATMENT OF V/STOL WALL INTERFERENCE FOR CLOSED CIRCULAR TUNNELS

By Harry H. Heyson
Langley Research Center

SUMMARY

An approximate treatment of V/STOL wall interference in a circular tunnel indicates that the interference factors at the model for this tunnel should be of the same order of magnitude as those presently available for a square tunnel of equal cross-sectional area. There is a greater degree of uncertainty with respect to the lateral and longitudinal distributions of interference; however, the available results for the square tunnel should be reasonably close to those of the circular tunnel provided that the model is relatively small in comparison with the test section.

INTRODUCTION

References 1 to 5 have provided theoretical treatments of wind-tunnel interference for V/STOL models in rectangular tunnels. As yet, however, there has been no equivalent treatment of such models in tunnels of circular cross section despite the fact that several such tunnels are regularly used for V/STOL studies both in this country and abroad.

References 1 to 5 obtained interference factors by the use of an external image system to represent the flat boundaries of the tunnels. In the case of a circular tunnel, only limited information can be obtained in this manner (for example, ref. 6); however, other techniques (refs. 7 and 8) can be used for solution of the complete three-dimensional problem. A start in this direction was made recently by Michel (ref. 9) who obtained the interference for a single doublet of arbitrary inclination and location within a circular tunnel; however, the study of reference 9 was never completed as the integrations required to extend the results to a complete wake were not carried out.

The present study does not attempt a rigorous treatment of the circular tunnel. Instead, two square sections of different orientation, the interference in which should bound the interference in the circular tunnel, are examined. The computed results should indicate the magnitude of the difference to be expected between circular and square test sections. In view of the approximate nature of the analysis, only centered vanishingly small models are considered herein.

SYMBOLS

Because of the limitations of the computer-controlled plotter used to prepare the figures, small variations in these symbols appear in the figures.

A_m momentum area of lifting system

A_T test-section cross-sectional area

$$A_1 = \sqrt{\left(\frac{x}{D}\right)^2 + \left(\frac{y}{D}\right)^2 + \left(\frac{z}{D}\right)^2}$$

$$A_2 = A_1 + \frac{z}{D} \cos \chi - \frac{x}{D} \sin \chi$$

C_L lift coefficient, Lift/qS

D semidiagonal length of square cross section

H semiheight of square tunnel

K function related to induced velocities of wake in free air

m, n integers

q dynamic pressure

R radius of tunnel with circular cross section

S wing area

t integer, equal to zero for lift forces and 1 for drag forces

u, v, w induced velocities directed parallel to X-, Y-, and Z-axis, respectively

u_0 mean value of longitudinal induced velocity

w_0 mean value of vertical induced velocity

x, y, z distances measured along the X-, Y-, and Z-axis, respectively

- X,Y,Z** Cartesian coordinate axes centered in model and tunnel; X-axis positive rearward, Z-axis positive upward, and the Y-axis oriented to form a right-hand coordinate system
- δ wind-tunnel interference factor defined in terms of momentum area and mean induced velocity; for example, $\Delta u_L = \delta_{u,L} \frac{A_m}{A_T} w_0$ and $\Delta w_D = \delta_{w,D} \frac{A_m}{A_T} u_0$
- $\Delta\alpha$ change in angle of attack caused by wall interference, radians
- χ wake skew angle, angle at which wake leaves the model, measured positive rearward from negative Z-axis to center of wake

Subscripts:

- u** pertaining to longitudinal velocities
- v** pertaining to lateral velocities
- w** pertaining to vertical velocities
- D** pertaining to drag forces
- L** pertaining to lift forces
- ∞ pertaining to a semi-infinite wake

THEORY

General Approach

The initial solution for a wind-tunnel interference problem was for the circular tunnel with a model having an undeflected wake (ref. 6). After obtaining the interference for this case, Prandtl noted that the interference in a square tunnel should be about the same as that in a circular tunnel of equal cross-sectional area. This assumption was later borne out when Glauert (ref. 10) obtained an interference factor (defined in this case

as $\delta = \frac{\Delta\alpha A_T}{SC_L}$ of 0.137 for a small model in the square tunnel as compared with the corresponding value of 0.125 obtained by Prandtl in the circular tunnel.

The situation becomes more complicated when the wake is deflected substantially downward from the horizontal. References 1 to 5 have indicated that for large deflections the interference factors increase and, furthermore, that the increase in interference is largely due to a greatly increased effect of the floor upon the phenomenon. Thus, it might be expected that the "floor" of the circular tunnel, being concave upward, would further increase the interference over that for the square tunnel. On the other hand, if the tunnels are of equal cross-sectional area (fig. 1), the lower regions of the circular tunnel are somewhat farther below the model than the floor of the equivalent square tunnel. The result of this increased distance should tend to counter to some degree the concavity of the circular tunnel.

If the square tunnel is now rotated 45° (to form what will be termed herein a diamond tunnel), it will be seen that the differences between the two square configurations are greater than the differences between the square and circular configurations. (Observe that the diamond section has a greater effective concavity of the floor than the circular configuration and that the center of the floor is farther from the model in the diamond section.) The advantage of considering the problem in this light is that the interference in both the square and diamond sections can be calculated from image systems with little mathematical difficulty. Once the interference factors for both rectangular configurations are available, it is reasonable to assume that the interference in the circular tunnel should lie within these factors. For convenience, the present study takes the interference factors for the circular tunnel to be the arithmetic mean of those for the square and diamond sections.

The Deflected Wake

The wake assumed herein is identical to that of reference 3. It originates at the model, passes downward and rearward in a straight line defined by the angle χ measured from the vertical tunnel axis. In free air, the wake continues to infinity. (See fig. 2(a).) In the tunnel, however, it meets the lower boundary. At this point (as in the upper half of fig. 2(b)), the wake is assumed to turn and flow off along the lower boundary. Although no real wake could behave in such a manner, the wake comprised of the two linear paths described appears to be a reasonable approximation to the actual curved path of the wake, at least for conditions which do not result in completely gross distortions of flow throughout the entire tunnel. (See refs. 11 and 12.)

The wake of the vanishingly small model considered herein is a simple doublet line wherein the axes of the doublets are inclined according to the induced drag-lift ratio of

the model. For convenience, the calculations are performed twice: once with the doublet axes vertical corresponding to pure lift forces; and once with the doublet axes horizontal corresponding to pure drag forces. Any arbitrary drag-lift ratio (or doublet inclination) can then be obtained by an appropriate superposition of the two results. This model is equally applicable to wings or more complicated devices such as rotors. (See ref. 13.)

Square Section

For the square test section, the analysis is identical to that of reference 3 and the interference factors can be obtained directly from that paper. As a computational convenience, however, the values given herein were obtained by the use of a subroutine in the computer program given in the appendix. This subroutine (square) is merely a specialization of the program given as appendix A of reference 5.

Diamond Section

Induced field in free air.- As noted previously, the wake assumed for the diamond tunnel is the same as that of reference 3. In the present usage, it is more convenient to nondimensionalize the expressions for the free-air wake in terms of the semidiagonal distance D across the tunnel. Thus for the centered model, the vertical induced velocity due to lift is

$$w_{\infty} = w_0 \frac{A_m}{A_T} \left[-\frac{1}{\pi} K_w \left(\frac{x}{D}, \frac{y}{D}, \frac{z}{D} \right) \right] \quad (1a)$$

where

$$K_w \left(\frac{x}{D}, \frac{y}{D}, \frac{z}{D} \right) = \frac{\left(\frac{x}{D} \right)^2 + \left(\frac{y}{D} \right)^2}{A_1^3 A_2} - \left(\frac{\frac{z}{D} + A_1 \cos \chi}{A_1 A_2} \right)^2 \quad (1b)$$

and, as a special case, when $\chi = 90^\circ$,

$$K_w \left[\begin{array}{l} \left(\frac{x}{D}, \frac{y}{D}, \frac{z}{D} \right) \\ \chi = 90^\circ \end{array} \right] = \frac{\left(\frac{x}{D} \right)^2 + \left(\frac{y}{D} \right)^2}{\left(A_1 - \frac{x}{D} \right) A_1^3} - \left[\frac{\frac{z}{D}}{\left(A_1 - \frac{x}{D} \right) A_1} \right]^2 \quad (1c)$$

Similarly, the longitudinal induced velocity due to lift becomes

$$u_{\infty} = w_0 \frac{A_m}{A_T} \left[-\frac{1}{\pi} K_u \left(\frac{x}{D}, \frac{y}{D}, \frac{z}{D} \right) \right] \quad (2a)$$

where

$$K_u\left(\frac{x}{D}, \frac{y}{D}, \frac{z}{D}\right) = -\frac{\frac{x}{D} \frac{z}{D}}{A_1^3 A_2} - \frac{\left(\frac{z}{D} + A_1 \cos \chi\right)\left(\frac{x}{D} - A_1 \sin \chi\right)}{A_1^2 A_2^2} \quad (2b)$$

and, as a special case, when $\chi = 90^\circ$

$$K_u \left|_{\chi = 90^\circ} \left(\frac{x}{D}, \frac{y}{D}, \frac{z}{D}\right) = \frac{z}{A_1^3 D} \quad (2c)$$

In the present derivation, the lateral induced velocities are also required. Thus, differentiating the free-air potential of the semi-infinite wake of vertical doublets with respect to y and then nondimensionalizing with respect to D yields

$$v_\infty = w_0 \frac{A_m}{A_T} \left[-\frac{1}{\pi} K_v\left(\frac{x}{D}, \frac{y}{D}, \frac{z}{D}\right) \right] \quad (3a)$$

where

$$K_v\left(\frac{x}{D}, \frac{y}{D}, \frac{z}{D}\right) = -\frac{y}{D} \left(\frac{\frac{z}{D}}{A_1^3 A_2} + \frac{\frac{z}{D} + A_1 \cos \chi}{A_1^2 A_2^2} \right) \quad (3b)$$

and, as a special case, when $\chi = 90^\circ$,

$$K_v \left|_{\chi = 90^\circ} \left(\frac{x}{D}, \frac{y}{D}, \frac{z}{D}\right) = -\frac{\frac{y}{D} \frac{z}{D}}{A_1^3 A_2^2} \left(2A_1 - \frac{x}{D}\right) \quad (3c)$$

The corresponding results for the wake of horizontal doublets are: The vertical induced velocity due to drag is

$$w_\infty = u_0 \frac{A_m}{A_T} \left[-\frac{1}{\pi} K_w\left(\frac{x}{D}, \frac{y}{D}, \frac{z}{D}\right) \right] \quad (4a)$$

where

$$K_w\left(\frac{x}{D}, \frac{y}{D}, \frac{z}{D}\right) = -\frac{\frac{x}{D} \frac{z}{D}}{A_1^3 A_2} - \frac{\left(\frac{z}{D} + A_1 \cos \chi\right)\left(\frac{x}{D} - A_1 \sin \chi\right)}{A_1^2 A_2^2} \quad (4b)$$

and, as a special case, when $\chi = 90^\circ$,

$$K_w \Big|_{\chi = 90^\circ} \left(\frac{x}{D}, \frac{y}{D}, \frac{z}{D} \right) = \frac{\frac{z}{D}}{A_1^3} \quad (4c)$$

The longitudinal induced velocity due to drag is

$$u_\infty = u_0 \frac{A_m}{A_T} \left[-\frac{1}{\pi} K_u \left(\frac{x}{D}, \frac{y}{D}, \frac{z}{D} \right) \right] \quad (5a)$$

where

$$K_u \left(\frac{x}{D}, \frac{y}{D}, \frac{z}{D} \right) = \frac{\left(\frac{y}{D} \right)^2 + \left(\frac{z}{D} \right)^2}{A_1^3 A_2} - \left(\frac{\frac{x}{D} - A_1 \sin \chi}{A_1 A_2} \right)^2 \quad (5b)$$

and, as a special case, when $\chi = 90^\circ$,

$$K_u \Big|_{\chi = 90^\circ} \left(\frac{x}{D}, \frac{y}{D}, \frac{z}{D} \right) = \frac{\frac{x}{D}}{A_1^3} \quad (5c)$$

The lateral induced velocity is obtained in a manner similar to equations (3) to obtain

$$v_\infty \left(\frac{x}{D}, \frac{y}{D}, \frac{z}{D} \right) = u_0 \frac{A_m}{A_T} \left[-\frac{1}{\pi} K_v \left(\frac{x}{D}, \frac{y}{D}, \frac{z}{D} \right) \right] \quad (6a)$$

where

$$K_v \left(\frac{x}{D}, \frac{y}{D}, \frac{z}{D} \right) = -\frac{y}{D} \left(\frac{\frac{x}{D}}{A_1^3 A_2} + \frac{\frac{x}{D} - A_1 \sin \chi}{A_1^2 A_2^2} \right) \quad (6b)$$

and, as a special case, when $\chi = 90^\circ$,

$$K_v \Big|_{\chi = 90^\circ} \left(\frac{x}{D}, \frac{y}{D}, \frac{z}{D} \right) = \frac{\frac{y}{D}}{A_1^3} \quad (6c)$$

Wake in the diamond test section.- Equations (1) to (6) provide only the induced velocity field of the semi-infinite wake in free air (fig. 2(a)). The field of the system in simple ground effect, under the present assumptions, can be obtained from the wake and image system indicated in figure 2(b). The field of the finite segment of inclined wake may be obtained by summing the fields of two semi-infinite wakes; one starting from the origin; the other, of equal but opposite strength, starting from the intersection of the original wake and the ground. The trailing leg of the wake also originates at the intersection with the ground and always has a skew angle of 90° .

The images below the ground, which are required in order to satisfy the condition of zero normal flow at the boundary, can be obtained in the same manner with suitable transpositions of the origin. Observe that a downwash with respect to the coordinate system of the image becomes an upwash with respect to the coordinate system of the real wake.

The wake and image pattern required to produce zero normal flow through the two planes corresponding to the bottom corner of the diamond tunnel is somewhat more complicated. (See fig. 2(c).) Observe that the symmetries required to meet the boundary conditions in the corner necessitate three images. Of these three images, the first is identical to the image in the ground-effect system. The remaining two images lie in a horizontal plane through the corner. Because of the 90° -rotation of these images with respect to the real wake, it is the lateral induced velocities of the images which contribute to the vertical induced velocity field of the real wake.

This fundamental cell of four wakes must be repeated in a doubly infinite pattern (as in fig. 2(d)) to satisfy conditions of zero normal flow through all four walls of the diamond section. Note that the basic unit of four cells repeats at intervals of $2(m-n)D$ in the Y-direction and at intervals of $2(m+n)D$ in the Z-direction. Thus, by defining the interference factors as in reference 3, the required superpositions yield

$$\begin{aligned}
\delta_{w,-} = & -\frac{1}{\pi} \left(\sum_{\substack{m=-\infty \\ m=n \neq 0}}^{\infty} \sum_{n=-\infty}^{\infty} K_w \left[\frac{x}{D}, \frac{y}{D} - 2(m-n), \frac{z}{D} - 2(m+n) \right] + \sum_{m=-\infty}^{\infty} \sum_{n=-\infty}^{\infty} \left\{ -K_w \left[\frac{x}{D} - \tan \chi, \frac{y}{D} - 2(m-n), \frac{z}{D} - 2(m+n) + 1 \right] \right. \right. \\
& - K_w \left[\frac{x}{D}, -\frac{y}{D} + 2(m-n), -\frac{z}{D} + 2(m+n) - 2 \right] + K_w \left[\frac{x}{D} - \tan \chi, -\frac{y}{D} + 2(m-n), -\frac{z}{D} + 2(m+n) - 1 \right] \\
& - K_v \left[\frac{x}{D}, -\frac{z}{D} + 2(m+n) - 1, \frac{y}{D} - 2(m-n) - 1 \right] + K_v \left[\frac{x}{D} - \tan \chi, -\frac{z}{D} + 2(m+n) - 1, \frac{y}{D} - 2(m-n) \right] \\
& + K_v \left[\frac{x}{D}, \frac{z}{D} - 2(m+n) + 1, -\frac{y}{D} + 2(m-n) - 1 \right] - K_v \left[\frac{x}{D} - \tan \chi, \frac{z}{D} - 2(m+n) + 1, -\frac{y}{D} + 2(m-n) \right] \\
& \left. \left. + 2tK_w \Big|_{\chi=90^\circ} \left[\frac{x}{D} - \tan \chi, \frac{y}{D} - 2(m-n), \frac{z}{D} - 2(m+n) + 1 \right] + 2tK_v \Big|_{\chi=90^\circ} \left[\frac{x}{D} - \tan \chi, \frac{z}{D} - 2(m+n) + 1, -\frac{y}{D} + 2(m-n) \right] \right\} \right) \quad (7)
\end{aligned}$$

where for $\delta_{w,L}$, K_w and K_v are from equations (1) and (3) and $t = 0$. For $\delta_{w,D}$, K_w and K_v are from equations (4) and (6) and $t = 1$.

$$\begin{aligned}
\delta_{u,-} = & -\frac{1}{\pi} \left(\sum_{\substack{m=0 \\ n=0 \\ m=n \neq 0}}^{\infty} K_u \left[\frac{x}{D}, \frac{y}{D} - 2(m-n), \frac{z}{D} - 2(m+n) \right] + \sum_{m=0}^{\infty} \sum_{n=0}^{\infty} \left\{ -K_u \left[\frac{x}{D} - \tan \chi, \frac{y}{D} - 2(m-n), \frac{z}{D} - 2(m+n) + 1 \right] \right. \right. \\
& + K_u \left[\frac{x}{D}, -\frac{y}{D} + 2(m-n), -\frac{z}{D} + 2(m+n) - 2 \right] - K_u \left[\frac{x}{D} - \tan \chi, -\frac{y}{D} + 2(m-n), -\frac{z}{D} + 2(m+n) - 1 \right] \\
& + K_u \left[\frac{x}{D}, -\frac{z}{D} + 2(m+n) - 1, \frac{y}{D} - 2(m-n) - 1 \right] - K_u \left[\frac{x}{D} - \tan \chi, -\frac{z}{D} + 2(m+n) - 1, \frac{y}{D} - 2(m-n) \right] \\
& + K_u \left[\frac{x}{D}, \frac{z}{D} - 2(m+n) + 1, -\frac{y}{D} + 2(m-n) - 1 \right] - K_u \left[\frac{x}{D} - \tan \chi, \frac{z}{D} - 2(m+n) + 1, -\frac{y}{D} + 2(m-n) \right] \\
& \left. \left. + 4tK_u \left[\frac{x}{D} - \tan \chi, \frac{y}{D} - 2(m-n), \frac{z}{D} - 2(m+n) + 1 \right] \right\} \right) \quad (8)
\end{aligned}$$

where, for $\delta_{u,L}$, K_u is from equations (2) and $t = 0$, and, where, for $\delta_{u,D}$, K_u is from equations (5) and $t = 1$.

When the wake passes directly rearward ($\chi = 90^\circ$), all the terms of equations (7) and (8) in which the x-dimension appears as $\frac{x}{D} - \tan \chi$ are zero and may be ignored in numerical calculations.

When $m = n = 0$, the first term represents the wake in free air. Observe that this term is omitted in equations (7) and (8) since it is desired that these equations represent only the additional interference caused by the walls.

Equations (7) and (8) represent the interference only in a closed tunnel. Equivalent expressions could be obtained for an open tunnel; however, as discussed in references 1 and 3, the assumptions inherent in the theory for that case would make the results of dubious validity.

Circular Tunnel

To approximate the circular tunnel, the interferences are assumed to be equal to the average interferences in square and diamond tunnels of equal cross-sectional area.

For equal areas, $\pi R^2 = 4H^2 = 2D^2$ so that

$$\left. \begin{aligned} \frac{H}{R} &= \frac{\sqrt{\pi}}{2} \\ \frac{D}{R} &= \sqrt{\frac{\pi}{2}} \end{aligned} \right\} \quad (9)$$

Thus, for any given value of x/R , y/R , and z/R in the circular tunnel, equations (9) may be used to convert the given coordinates for proper entry into the equations

of reference 3 or 5 for the square tunnel or into equations (7) and (8) of the present paper for the diamond tunnel. After calculating both sets of interference factors, the average values are assumed to represent the interference factors for the circular tunnel. A FORTRAN program for performing the calculations is presented in the appendix.

RESULTS AND DISCUSSION

Interference at the Model

Figure 3 compares the interference factors at the model for all three tunnels. At the higher wake angles, the interference factors for vertical interference are somewhat larger in magnitude in the round tunnel than in the square tunnel; whereas, the reverse is true at very low skew angles. This result is in accordance with the previously anticipated trends. The factor for horizontal interference due to lift $\delta_{u,L}$ is always somewhat less in the round tunnel and the factor for horizontal interference due to drag $\delta_{u,D}$ is always more negative in the round tunnel than in the square tunnel.

Two considerations should be noted carefully when the interference factors presented in figure 3 are examined. First, an effective wake angle should be used in applying the results in order to account for the effect of wake rollup on the inclination of the wake (refs. 13 and 14), and this effective wake angle results in a substantial increase in χ . Secondly, it has been shown experimentally (refs. 11 and 15) and theoretically (ref. 12) that there is a minimum value of χ , which can be tolerated in V/STOL testing, beyond which the flow in the tunnel is so distorted that the measured data become meaningless. Thus, in a practical sense, it is only necessary to consider the reasonably large values of χ . Under these circumstances, examination of figure 3 indicates that the interference in the round tunnel will not be greatly different from that in the square tunnel. For most practical cases, the interference factors will differ by only about 10 percent between the two tunnels. Thus, if the model is reasonably small, with a span on the order of one-fourth or one-third of the tunnel diameter, it should be completely satisfactory to use the interference factors for a square tunnel. Indeed, this procedure is quite attractive since detailed computer programs applicable to the square tunnel are available. (See refs. 4 and 5.)

At a wake angle of 90° , the present result for the square tunnel is $\delta_{w,L} = -0.545$ and for the diamond tunnel is $\delta_{w,L} = -0.547$. Because of the different definitions of the interference factors, it is necessary to divide these values by -4 (ref. 3) before comparing them with Glauert's value of 0.137 for the square tunnel. The aforementioned division leads to satisfactory agreement with Glauert's result when the differing degrees of numerical approximation are considered. It is interesting to note that there is no significant difference between the interferences in the square and diamond sections when the

wake is undeflected ($\chi = 90^\circ$). In either case, the interference obtained is within about 10 percent of Prandtl's (ref. 6) exact value of 0.125 for the circular tunnel.

Interference Along Longitudinal Axis

Similar comparisons are shown for the longitudinal distribution of interference along the tunnel axis in figures 4 to 7. Not all the computed points are shown; the curves are drawn from calculations made at 29 values of x/R . For typical tail lengths, on the order of $1/2 R$ to R , examination of these figures indicates that corrections at the tail for pitching moment may be somewhat less satisfactory than those at the center of lift if the factors for a square tunnel are applied to tests in a circular tunnel. The error will be reduced, however, as the wake angle increases toward 90° , and such correction is obviously superior to no correction at all.

Interference Along Lateral Axis

Equivalent comparisons on the lateral axis of the tunnel are shown in figures 8 to 11. The curves are drawn from calculations made at 13 values of y/R . In general, the trends of the distribution over this axis of the factors related to longitudinal interference are about the same; the major difference being in the overall level of interference. Unfortunately, the interference in the square and diamond test sections tends to produce opposite trends in the lateral distribution of the interference factors related to the vertical interference velocity; the differences become greater as the wake skew angle increases. The approximate solution for the circular tunnel is rather uniform because it is taken merely as the average of the square and diamond sections. The sensitivity of the result to the sidewall configuration leaves some doubt that similar uniform results would be obtained for a finite-span system, the representation of which would require laterally offset elemental wakes (ref. 4). Thus, the present results should be construed as applying only to lifting systems of small lateral extent.

CONCLUDING REMARKS

An approximate treatment of V/STOL wall interference in a circular tunnel indicates that the interference factors at the model for this tunnel should be of the same order of magnitude as those presently available for a square tunnel of equal cross-sectional area. There is a greater degree of uncertainty with respect to the lateral and longitudinal distributions of interference; however, the available results for the square

tunnel should be reasonably close to those of the circular tunnel provided that the model is relatively small in comparison with the test section.

Langley Research Center,
National Aeronautics and Space Administration,
Hampton, Va., December 31, 1970.

APPENDIX

FORTRAN PROGRAM FOR APPROXIMATING THE WIND-TUNNEL INTERFERENCE FOR A SMALL MODEL IN A CIRCULAR TUNNEL

THIS PROGRAM WAS WRITTEN IN CDC FORTRAN, VERSION 2.1, TO RUN ON CDC 6000 SERIES COMPUTERS WITH THE SCOPE 3.0 OPERATING SYSTEM AND LIBRARY TAPE. MINOR MODIFICATIONS MAY BE REQUIRED PRIOR TO USE IN OTHER COMPUTERS. THIS PROGRAM HAS BEEN FOUND SATISFACTORY ON THE AFOREMENTIONED COMPUTERS WHICH CARRY THE EQUIVALENT OF APPROXIMATELY 15 DECIMAL DIGITS. COMPUTERS OF LESSER PRECISION MAY REQUIRE MODIFICATION TO DOUBLE PRECISION IN ORDER TO OBTAIN RESULTS OF EQUAL NUMERICAL ACCURACY.

TWO SUBROUTINES ARE USED. SUBROUTINE <SQUARE> IS A MODIFICATION OF THE PROGRAM GIVEN AS APPENDIXES A AND C OF NASA TECHNICAL MEMORANDUM X-1740. IT COMPUTES THE INTERFERENCE FACTORS FOR A SQUARE, CLOSED TEST SECTION. SUBROUTINE <DIAMOND> IS A FORTRAN CODING OF EQUATIONS (7) AND (8) OF THE PRESENT PAPER. CONVERSIONS BETWEEN NONDIMENSIONALIZATIONS WITH RESPECT TO R, H, AND D ARE MADE IN THE APPROPRIATE ROUTINES.

THE REQUIRED INPUT, FOUND AT ADDRESS 1 (LINE (A 9)) IN FORMAT 103 (LINE (A 40)), CONSISTS ONLY OF THE X-, Y-, AND Z-DISTANCES FROM THE MODEL TO THE POINT AT WHICH THE INTERFERENCE FACTORS ARE REQUIRED. ALL THREE DISTANCES MUST BE NONDIMENSIONALIZED WITH RESPECT TO THE RADIUS OF THE CIRCULAR TEST SECTION.

```

PROGRAM KCLND (INPUT,OUTPUT,TAPE5=INPUT,TAPE6=OUTPUT)          (A 1)
C                                                                    (A 2)
C                                                                    (A 3)
COMMON XOVERH,YOVERH,ZOVERH,DELTA(4)                            (A 4)
DIMENSION DELTA1(4),DELTA2(4),NAME(4),C(11)                     (A 5)
DATA (NAME(I),I=1,4)/1CHDELTA(W,L),1OHDELTA(U,L),1OHDELTA(W,C),1OH- (A 6)
1DELTA(U,L)/                                                    (A 7)
DATA (C(I),I=1,11)/-3.,3.,10.,20.,30.,40.,50.,60.,70.,80.,9C./ (A 8)
1 READ (5,103) XCVERR,YOVERR,ZOVERR                             (A 9)
IF (EOF,5) 999,2                                               (A 10)
2 PI=3.14159265358979                                          (A 11)
HCVERR=SQRT(PI/4.)                                             (A 12)
XOVERH=XCVERR/HCVERR                                          (A 13)
YOVERH=YOVERR/HCVERR                                          (A 14)
ZOVERH=ZOVERR/HCVERR                                          (A 15)
WRITE (6,148) XOVERH,YOVERR,ZOVERR                             (A 16)
WRITE (6,150)                                                  (A 17)
DO 41 K=1,11                                                    (A 18)
WRITE (6,149) C(K)                                             (A 19)
DO 20 I=1,4                                                     (A 20)
20 DELTA(I)=DELTA1(I)=DELTA2(I)=C.                              (A 21)
C                                                                    (A 22)
C                                                                    (A 23)
CALL SQUARE ((K))                                              (A 24)
C                                                                    (A 25)
C                                                                    (A 26)
DO 3 I=1,4                                                      (A 27)
3 DELTA1(I)=DELTA(I)                                           (A 28)
C                                                                    (A 29)
C                                                                    (A 30)
CALL DIAMOND (C(K))                                            (A 31)
C                                                                    (A 32)

```

APPENDIX — Continued

```

C
  DC 4   I=1,4                                (A 33)
  DELTA2(I)=DELTA(I)                          (A 34)
  4 DELTA(I)=(DELTA1(I)+DELTA(I))/2.          (A 35)
  WRITE (6,151) ((NAME(I),DELTA1(I),DELTA2(I),DELTA(I)),I=1,4) (A 36)
41 CONTINUE
  GC TO 1                                       (A 37)
  GC TO 1                                       (A 38)
  GC TO 1                                       (A 39)
103 FORMAT (3F10.3)                            (A 40)
148 FORMAT (1F1//23X*INTERFERENCE FACTORS AT A POINT NEAR A VANISHINGL (A 41)
  1Y SMALL MODEL*//32X*APPROXIMATE SOLUTION IN A ROUND CLOSED TUNNEL* (A 42)
  2 //23X*X/R =*F8.3,9X*Y/R =*F8.3,11X*Z/R =*F8.3//) (A 43)
149 FORMAT (/8X*CHI =*F7.3/)                  (A 44)
150 FORMAT (22X*SQUARE TUNNEL*19X*DIAMOND TUNNEL*15X*AVERAGE (ROUND TU (A 45)
  2NNEL)*//22X,13(1F=),19X,14(1F=),15X,22(1F=)) (A 46)
151 FORMAT (1CX,A1C,F12.4,2F32.4)            (A 47)
999 STOP                                       (A 48)
  END                                           (A 49)

SUBROUTINE DIAMOND (ANGL)                      (A 50)
  COMMON XCOVER, YCOVER, ZCOVER, DELTA(4)     (A 51)
  DIMENSION V(4)                              (A 52)
  SC=SIN(ANGL*0.0174532925199)                (A 53)
  CC=COS(ANGL*0.0174532925199)                (A 54)
  XOVERD=XCOVER/SQRT(2.0)                     (A 55)
  YOVERD=YCOVER/SQRT(2.0)                     (A 56)
  ZOVERD=ZCOVER/SQRT(2.0)                     (A 57)
  DO 1 I=1,28                                  (A 58)
1  DELTA(I)=C.C                                (A 59)
  DO 2 IM=1,7                                   (A 60)
  DO 2 IN=1,7                                   (A 61)
  DO 3 I=1,4                                    (A 62)
3  V(I)=0.0                                     (A 63)
  M=2.*(IM-IN)                                  (A 64)
  N=2.*(IN+IM-8)                                (A 65)
  IF (IM.EQ.4.AND.IN.EQ.4) GO TO 4             (A 66)
  X=XCOVERC                                     (A 67)
  Y=YCOVERC-M                                   (A 68)
  Z=ZCOVERC-N                                   (A 69)
  A=SQRT(X*X+Y*Y+Z*Z)                          (A 70)
  B=A+Z*CC-X*SC                                  (A 71)
  V(1)=((X*X+Y*Y)/(B*A*A*A))-((Z+A*CC)/(B*A))*2 (A 72)
  V(2)=V(3)=-((X*Z)/(B*A*A*A)-(Z+A*CC)*(X-A*SC)/(B*B*A*A) (A 73)
  V(4)=((Y*Y+Z*Z)/(B*A*A*A))-((X-A*SC)/(B*A))*2 (A 74)
  DC 5 I=1,4                                    (A 75)
5  DELTA(I)=DELTA(I)+V(I)                      (A 76)
4  IF (ANGL.EQ.90.) GO TO 6                    (A 77)
  X=XCOVERC-(SC/CC)                             (A 78)
  Y=YCOVERC-M                                   (A 79)
  Z=ZCOVERC-N+1.                                (A 80)
  A=SQRT(X*X+Y*Y+Z*Z)                          (A 81)
  B=A+Z*CC-X*SC                                  (A 82)
  V(1)=((X*X+Y*Y)/(B*A*A*A))-((Z+A*CC)/(B*A))*2 (A 83)
  V(2)=V(3)=-((X*Z)/(B*A*A*A)-(Z+A*CC)*(X-A*SC)/(B*B*A*A) (A 84)
  V(4)=((Y*Y+Z*Z)/(B*A*A*A))-((X-A*SC)/(B*A))*2 (A 85)
  DC 7 I=1,4                                    (A 86)
7  DELTA(I)=DELTA(I)-V(I)                      (A 87)
6  X=XCOVERC                                     (A 88)
  Y=-YOVERD+M                                   (A 89)
  Z=-ZCOVERD+N-2.                               (A 90)
  A=SQRT(X*X+Y*Y+Z*Z)                          (A 91)
  B=A+Z*CC-X*SC                                  (A 92)

```

APPENDIX - Continued

```

V(1) = ((X*)+Y*Y)/(B*A*A*A) - ((Z+A*CC)/(B*A))**2 (A 93)
V(2) = V(3) = -(X*Z)/(B*A*A*A) - (Z+A*CC)*(X-A*SC)/(B*B*A*A) (A 94)
V(4) = ((Y*Y+Z*Z)/(B*A*A*A) - ((X-A*SC)/(B*A))**2 (A 95)
DO 8 I=1,4 (A 96)
8 DELTA(I) = DELTA(I) + ((-1.))**I * V(I) (A 97)
IF (ANGL.EC.9C.) GC TO 9 (A 98)
X = XOVERC - (SC/CC) (A 99)
Z = Z+1. (A 100)
A = SQRT(X*X+Y*Y+Z*Z) (A 101)
B = A+Z*CC-X*SC (A 102)
V(1) = ((X*)+Y*Y)/(B*A*A*A) - ((Z+A*CC)/(B*A))**2 (A 103)
V(2) = V(3) = -(X*Z)/(B*A*A*A) - (Z+A*CC)*(X-A*SC)/(B*B*A*A) (A 104)
V(4) = ((Y*Y+Z*Z)/(B*A*A*A) - ((X-A*SC)/(B*A))**2 (A 105)
DO 10 I=1,4 (A 106)
10 DELTA(I) = DELTA(I) - ((-1.))**I * V(I) (A 107)
9 X = XOVERC (A 108)
Y = -ZOVERC + N - 1. (A 109)
Z = YOVERC - M - 1. (A 110)
A = SQRT(X*X+Y*Y+Z*Z) (A 111)
B = A+Z*CC-X*SC (A 112)
V(1) = -Y*(Z+A*CC)/(A*A*B*B) - Y*Z/(B*A*A*A) (A 113)
V(2) = -(X*Z)/(B*A*A*A) - (Z+A*CC)*(X-A*SC)/(B*B*A*A) (A 114)
V(3) = -Y*(X-A*SC)/(A*A*B*B) - Y*X/(B*A*A*A) (A 115)
V(4) = ((Y*Y+Z*Z)/(B*A*A*A) - ((X-A*SC)/(B*A))**2 (A 116)
DO 11 I=1,4 (A 117)
11 DELTA(I) = DELTA(I) + ((-1.))**I * V(I) (A 118)
IF (ANGL.EC.9C.) GC TO 12 (A 119)
X = XOVERC - (SC/CC) (A 120)
Z = Z+1. (A 121)
A = SQRT(X*X+Y*Y+Z*Z) (A 122)
B = A+Z*CC-X*SC (A 123)
V(1) = -Y*(Z+A*CC)/(A*A*B*B) - Y*Z/(B*A*A*A) (A 124)
V(2) = -(X*Z)/(B*A*A*A) - (Z+A*CC)*(X-A*SC)/(B*B*A*A) (A 125)
V(3) = -Y*(X-A*SC)/(A*A*B*B) - Y*X/(B*A*A*A) (A 126)
V(4) = ((Y*Y+Z*Z)/(B*A*A*A) - ((X-A*SC)/(B*A))**2 (A 127)
DO 13 I=1,4 (A 128)
13 DELTA(I) = DELTA(I) - ((-1.))**I * V(I) (A 129)
12 X = XOVERC (A 130)
Y = ZOVERC - N + 1. (A 131)
Z = -YOVERC + M - 1. (A 132)
A = SQRT(X*X+Y*Y+Z*Z) (A 133)
B = A+Z*CC-X*SC (A 134)
V(1) = -Y*(Z+A*CC)/(A*A*B*B) - Y*Z/(B*A*A*A) (A 135)
V(2) = -(X*Z)/(B*A*A*A) - (Z+A*CC)*(X-A*SC)/(B*B*A*A) (A 136)
V(3) = -Y*(X-A*SC)/(A*A*B*B) - Y*X/(B*A*A*A) (A 137)
V(4) = ((Y*Y+Z*Z)/(B*A*A*A) - ((X-A*SC)/(B*A))**2 (A 138)
DO 14 I=1,4 (A 139)
14 DELTA(I) = DELTA(I) + V(I) (A 140)
IF (ANGL.EC.9C.) GC TO 2 (A 141)
X = XOVERC - (SC/CC) (A 142)
Z = Z+1. (A 143)
A = SQRT(X*X+Y*Y+Z*Z) (A 144)
B = A+Z*CC-X*SC (A 145)
V(1) = -Y*(Z+A*CC)/(A*A*B*B) - Y*Z/(B*A*A*A) (A 146)
V(2) = -(X*Z)/(B*A*A*A) - (Z+A*CC)*(X-A*SC)/(B*B*A*A) (A 147)
V(3) = -Y*(X-A*SC)/(A*A*B*B) - Y*X/(B*A*A*A) (A 148)
V(4) = ((Y*Y+Z*Z)/(B*A*A*A) - ((X-A*SC)/(B*A))**2 (A 149)
DO 15 I=1,4 (A 150)
15 DELTA(I) = DELTA(I) - V(I) (A 151)
Y = YOVERC - M (A 152)
Z = ZOVERC - N + 1. (A 153)
A = SQRT(X*X+Y*Y+Z*Z) (A 154)

```

APPENDIX – Continued

```

B=A-X (A 155)
V(3)=Z/(A*A*A) (A 156)
V(4)=X/(A*A*A) (A 157)
DC 16 I=3,4 (A 158)
16 DELTA(I)=DELTA(I)+4.*V(I) (A 159)
2 CONTINUE (A 160)
DO 19 I=1,4 (A 161)
19 DELTA(I)=-DELTA(I)/3.14159265358979 (A 162)
RETURN $END (A 163)

```

```

SUBROUTINE SQUARE (ANGL) (A 164)
COMMON XOVERH,YCOVERH,ZOVERH,DELTA(4) (A 165)
DIMENSION V(3,9),ADEL(4) (A 166)
SC=SIN(ANGL*.0174532925199) (A 167)
CC=COS(ANGL*.0174532925199) (A 168)
Z6= ZOVERH+1. (A 169)
Z8=-Z6 (A 170)
Z7=Z8-1. (A 171)
DC 8 J1=1,4 (A 172)
8 DELTA(J1)=C. (A 173)
DO 10 M=1,7 (A 174)
DO 10 N=1,7 (A 175)
IF (N.EQ.4.AND.M.EQ.4) GO TO 10 (A 176)
DC 11 J1=1,3 (A 177)
DO 11 J2=1,5 (A 178)
11 V(J1,J2)=0. (A 179)
DO 12 J1=1,4 (A 180)
12 ADEL(J1)=C. (A 181)
AM=M-4 (A 182)
AN=N-4 (A 183)
X= XOVERH (A 184)
Y= YCOVERH-2.*AM (A 185)
Z= (ZOVERH-4.*AN) (A 186)
A=SQRT(X*X+Y*Y+Z*Z) (A 187)
B=A+Z*CC-X*SC (A 188)
V(1,1)={{(X*X+Y*Y)/(B*A*A*A)}-((Z+A*CC)/(B*A))**2} (A 189)
V(2,1)=-{(X*Z)/(B*A*A*A)-(Z+A*CC)*(X-A*SC)/(B*B*A*A)} (A 190)
V(3,1)={{(Y*Y+Z*Z)/(B*A*A*A)}-((X-A*SC)/(B*A))**2} (A 191)
Z=-Z-2. (A 192)
A=SQRT(X*X+Y*Y+Z*Z) (A 193)
B=A+Z*CC-X*SC (A 194)
V(1,3)={{(X*X+Y*Y)/(B*A*A*A)}-((Z+A*CC)/(B*A))**2} (A 195)
V(2,3)=-{(X*Z)/(B*A*A*A)-(Z+A*CC)*(X-A*SC)/(B*B*A*A)} (A 196)
V(3,3)={{(Y*Y+Z*Z)/(B*A*A*A)}-((X-A*SC)/(B*A))**2} (A 197)
IF (ANGL.EQ.90.C) GO TO 13 (A 198)
X=X-(SC/CC) (A 199)
Z=-Z-1. (A 200)
A=SQRT(X*X+Y*Y+Z*Z) (A 201)
B=A+Z*CC-X*SC (A 202)
V(1,2)={{(X*X+Y*Y)/(B*A*A*A)}-((Z+A*CC)/(B*A))**2} (A 203)
V(2,2)=-{(X*Z)/(B*A*A*A)-(Z+A*CC)*(X-A*SC)/(B*B*A*A)} (A 204)
V(3,2)={{(Y*Y+Z*Z)/(B*A*A*A)}-((X-A*SC)/(B*A))**2} (A 205)
B=A-X (A 206)
V(1,5)={{(X*X+Y*Y)/(B*A*A*A)}-(Z/(B*A))**2} (A 207)
V(2,5)=Z/(A*A*A) (A 208)
V(3,5)=X/(A*A*A) (A 209)
Z=-Z (A 210)
B=A+Z*CC-X*SC (A 211)
V(1,4)={{(X*X+Y*Y)/(B*A*A*A)}-((Z+A*CC)/(B*A))**2} (A 212)
V(2,4)=-{(X*Z)/(B*A*A*A)-(Z+A*CC)*(X-A*SC)/(B*B*A*A)} (A 213)

```

APPENDIX – Concluded

```

V(3,4)=((Y*Y+Z*Z)/(B*A*A*A))-((X-A*SC)/(B*A))**2 (A 214)
13 ADEL(1)=V(1,1)-V(1,2)-V(1,3)+V(1,4) (A 215)
ADEL(2)=V(2,1)-V(2,2)+V(2,3)-V(2,4) (A 216)
ADEL(3)=V(2,1)-V(2,2)-V(2,3)+V(2,4)+2.*V(2,5) (A 217)
ADEL(4)=V(3,1)-V(3,2)+V(3,3)-V(3,4)+2.*V(3,5) (A 218)
DO 14 J1=1,4 (A 219)
14 DELTA(J1)=DELTA(J1)+ADEL(J1) (A 220)
10 CONTINUE (A 221)
X= XGVERH (A 222)
Y= YGVERH (A 223)
Z=Z7 (A 224)
A=SQRT(X*X+Y*Y+Z*Z) (A 225)
B=A+Z*CC-X*SC (A 226)
V(1,7)=((X*X+Y*Y)/(B*A*A*A))-((Z+A*CC)/(B*A))**2 (A 227)
V(2,7)=-((X*Z)/(B*A*A*A)-(Z+A*CC)*(X-A*SC)/(B*B*A*A) (A 228)
V(3,7)=((Y*Y+Z*Z)/(B*A*A*A))-((X-A*SC)/(B*A))**2 (A 229)
IF (ANGL.EC.9C.C) GO TO 16 (A 230)
X=X-(SC/CC) (A 231)
Z=Z6 (A 232)
A=SQRT(X*X+Y*Y+Z*Z) (A 233)
B=A+Z*CC-X*SC (A 234)
V(1,6)=((X*X+Y*Y)/(B*A*A*A))-((Z+A*CC)/(B*A))**2 (A 235)
V(2,6)=-((X*Z)/(B*A*A*A)-(Z+A*CC)*(X-A*SC)/(B*B*A*A) (A 236)
V(3,6)=((Y*Y+Z*Z)/(B*A*A*A))-((X-A*SC)/(B*A))**2 (A 237)
B=A-X (A 238)
V(1,9)=((X*X+Y*Y)/(B*A*A*A))-((Z/(B*A))**2 (A 239)
V(2,9)=Z/(A*A*A) (A 240)
V(3,9)=X/(A*A*A) (A 241)
Z=Z8 (A 242)
B=A+Z*CC-X*SC (A 243)
V(1,8)=((X*X+Y*Y)/(B*A*A*A))-((Z+A*CC)/(B*A))**2 (A 244)
V(2,8)=-((X*Z)/(B*A*A*A)-(Z+A*CC)*(X-A*SC)/(B*B*A*A) (A 245)
V(3,8)=((Y*Y+Z*Z)/(B*A*A*A))-((X-A*SC)/(B*A))**2 (A 246)
16 ADEL(1)=-V(1,6)-V(1,7)+V(1,8) (A 247)
ADEL(2)=-V(2,6)+V(2,7)-V(2,8) (A 248)
ADEL(3)=-V(2,6)-V(2,7)+V(2,8)+2.*V(2,9) (A 249)
ADEL(4)=-V(3,6)+V(3,7)-V(3,8)+2.*V(3,9) (A 250)
DO 17 J1=1,4 (A 251)
17 DELTA(J1)=DELTA(J1)+ADEL(J1) (A 252)
AMT=-2. /3.14159265358979 (A 253)
DO 19 J1=1,4 (A 254)
19 DELTA(J1)=AMT*DELTA(J1) (A 255)
RETURN (A 256)
END (A 257)

```

REFERENCES

1. Heyson, Harry H.: Jet-Boundary Corrections for Lifting Rotors Centered in Rectangular Wind Tunnels. NASA TR R-71, 1960.
2. Heyson, Harry H.: Wind-Tunnel Wall Interference and Ground Effect for VTOL-STOL Aircraft. J. Amer. Helicopter Soc., vol. 6, no. 1, Jan. 1961, pp. 1-9.
3. Heyson, Harry H.: Linearized Theory of Wind-Tunnel Jet-Boundary Corrections and Ground Effect for VTOL-STOL Aircraft. NASA TR R-124, 1962.
4. Heyson, Harry H.: Use of Superposition in Digital Computers To Obtain Wind-Tunnel Interference Factors for Arbitrary Configurations, With Particular Reference to V/STOL Models. NASA TR R-302, 1969.
5. Heyson, Harry H.: FORTRAN Programs for Calculating Wind-Tunnel Boundary Interference. NASA TM X-1740, 1969.
6. Prandtl, L.: Applications of Modern Hydrodynamics to Aeronautics. NACA Rep. 116, 1921.
7. Lotz, Irmgard: Correction of Downwash in Wind Tunnels of Circular and Elliptic Sections. NACA TM 801, 1936.
8. Joppa, Robert G.: A Method of Calculating Wind Tunnel Interference Factors for Tunnels of Arbitrary Cross Section. NASA CR-845, 1967.
9. Michel, P.: Effet de paroi sur un rotor d'helicoptere en veine fermée de section circulaire: Ecoulement incompressible autour d'un doublet placé dans une veine fermee circulaire. Doc. No. 12/2751 GN, Office National d'Etudes et de Recherches Aerospatiales, Nov. 1968, pp. 1-78, I-XXVII.
10. Glauert, H.: The Elements of Aerofoil and Airscrew Theory. Second ed., Cambridge Univ. Press, 1947. (Reprinted 1948.)
11. Rae, William H., Jr.: Limits on Minimum-Speed V/STOL Wind-Tunnel Tests. J. Aircraft, vol. 4, no. 3, May-June 1967, pp. 249-254.
12. Heyson, Harry H.: Theoretical Study of Conditions Limiting V/STOL Testing in Wind Tunnels With Solid Floor. NASA TN D-5819, 1970.
13. Heyson, Harry H.: The Flow Throughout a Wind Tunnel Containing a Rotor With a Sharply Deflected Wake. Proceedings Third CAL/AVLABS Symposium, Aerodynamics of Rotary Wing and V/STOL Aircraft, Vol. II, June 1969.
14. Heyson, Harry H.; and Grunwald, Kalman J.: Wind Tunnel Boundary Interference for V/STOL Testing. Conference on V/STOL and STOL Aircraft, NASA SP-116, 1966, pp. 409-434.

15. Rae, William H., Jr.; and Shindo, Shojiro: Comments on V/STOL Wind Tunnel Data at Low Forward Speeds. Proceedings Third CAL/AVLABS Symposium, Aerodynamics of Rotary Wing and V/STOL Aircraft, Vol. II, June 1969.

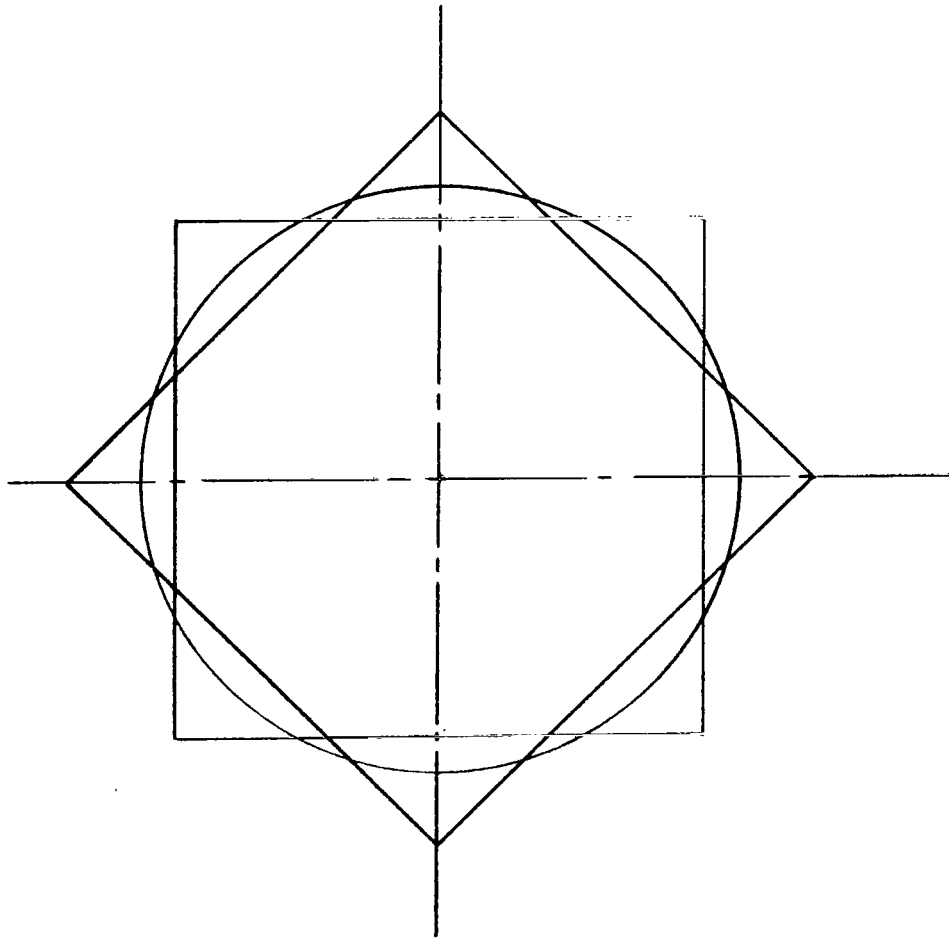
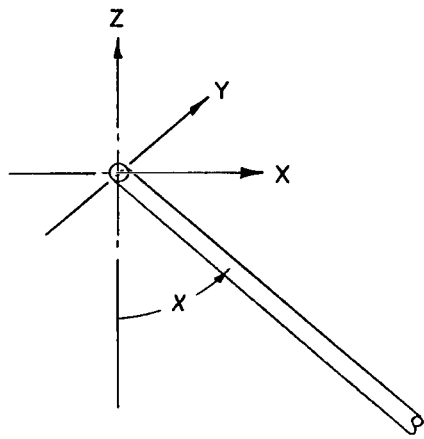
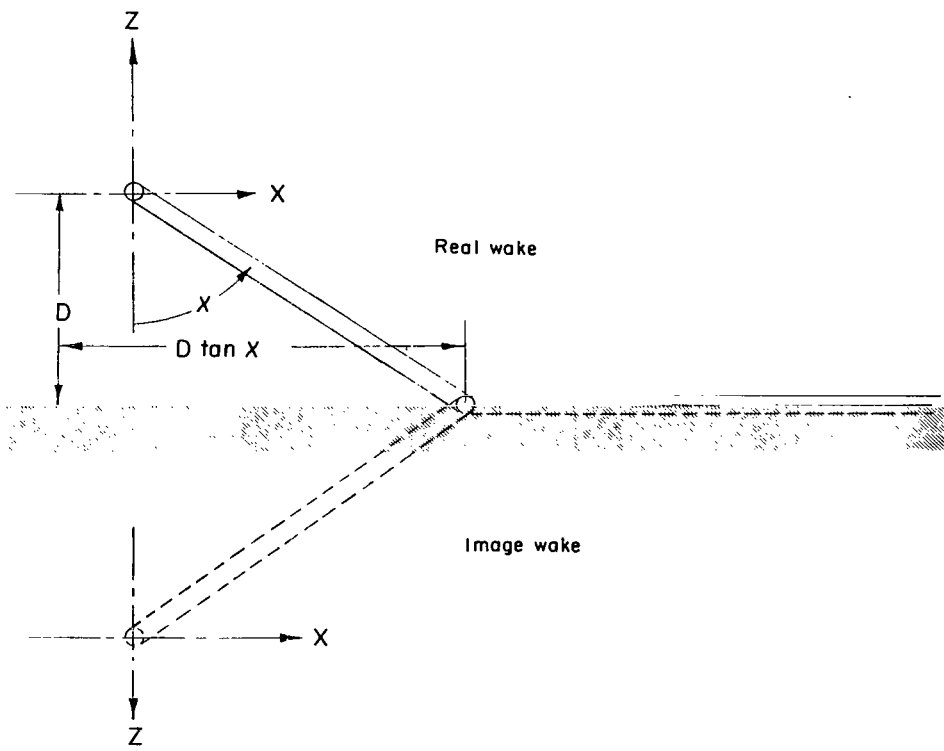


Figure 1.- Comparison of square, diamond, and circular test sections of equal cross-sectional area.

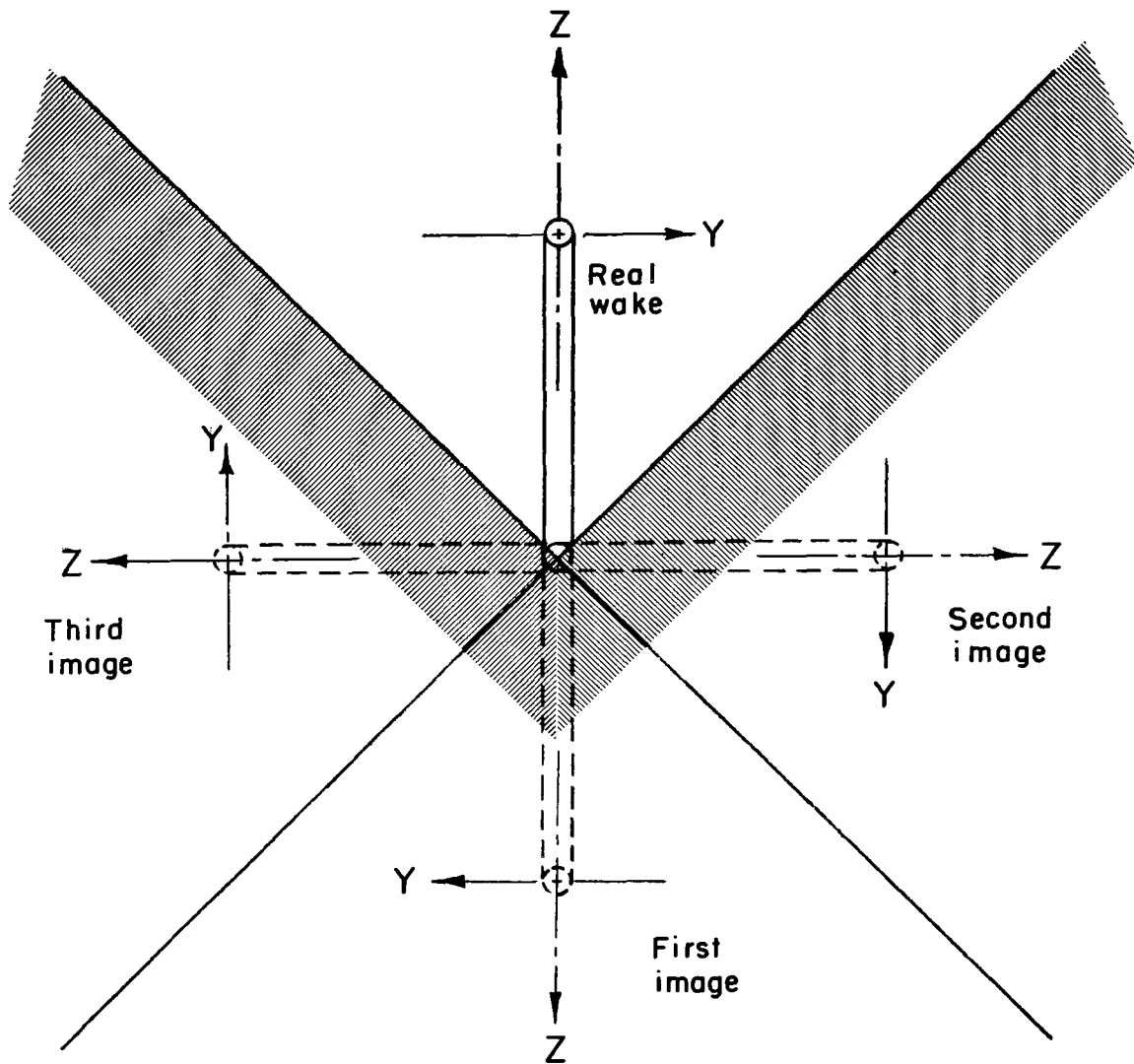


(a) Wake in free air.



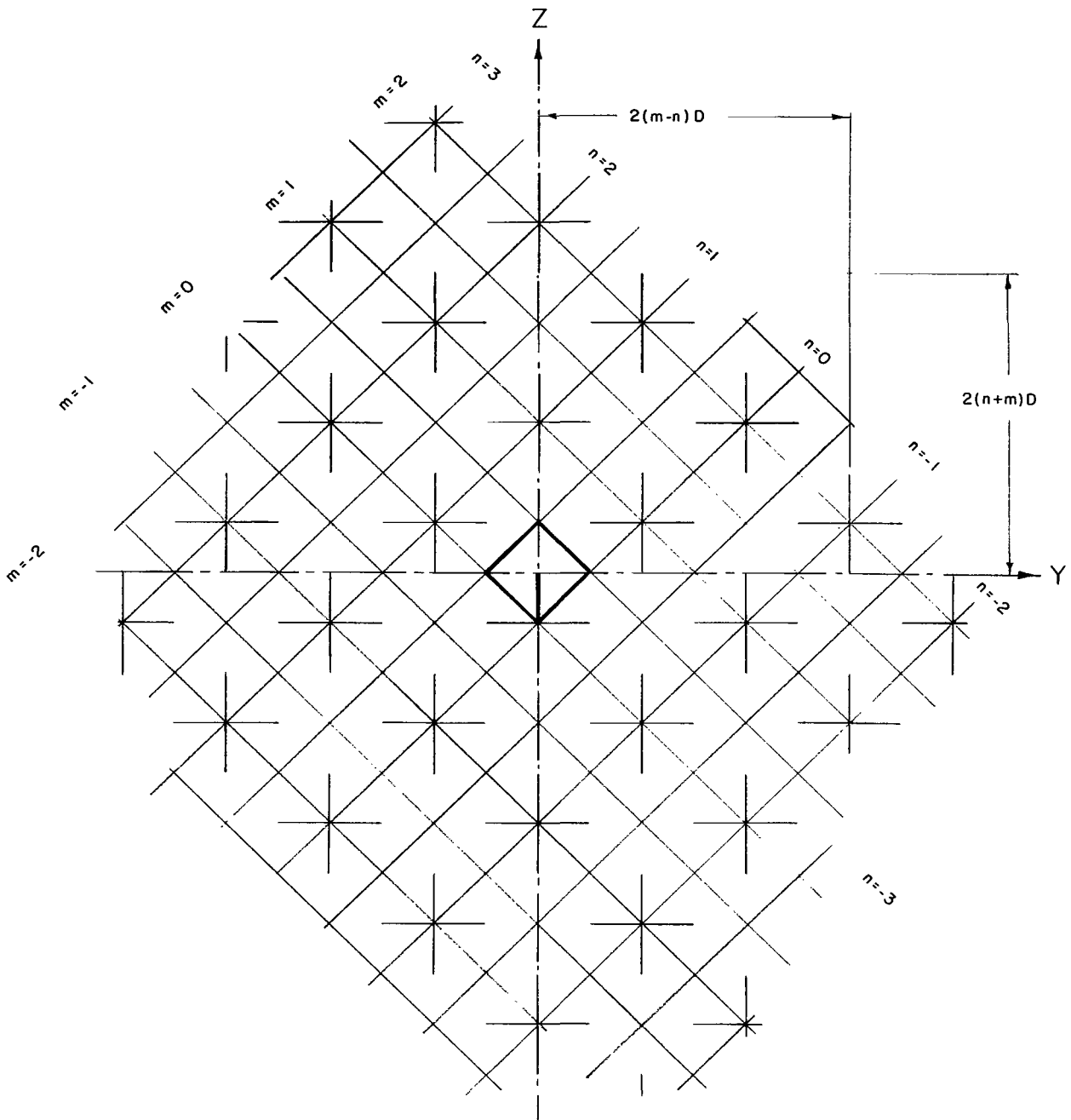
(b) Wake and image in ground effect.

Figure 2.- Wake and image systems used in developing interference factors for a diamond test section.



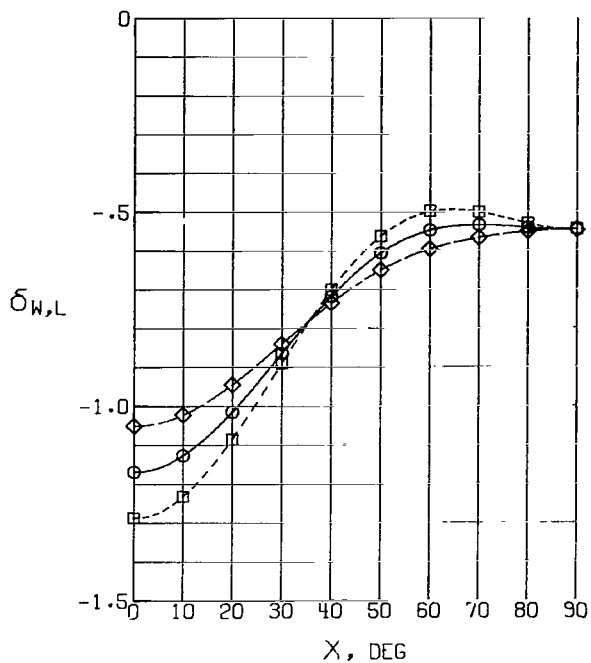
(c) Wake and images to represent a corner.

Figure 2.- Continued.

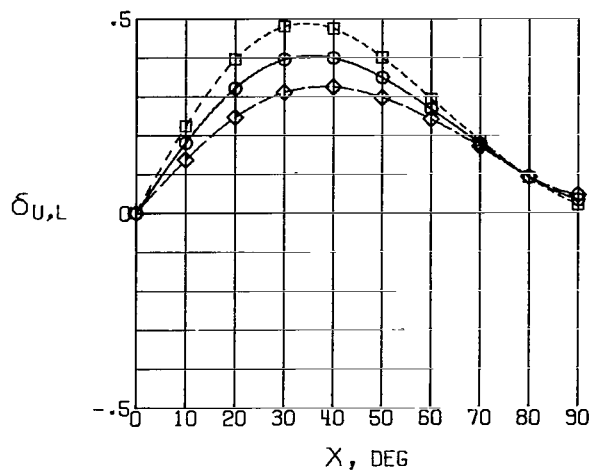


(d) Central portion of reflection system used to obtain interference factors in a diamond test section. Real tunnel is darkened.

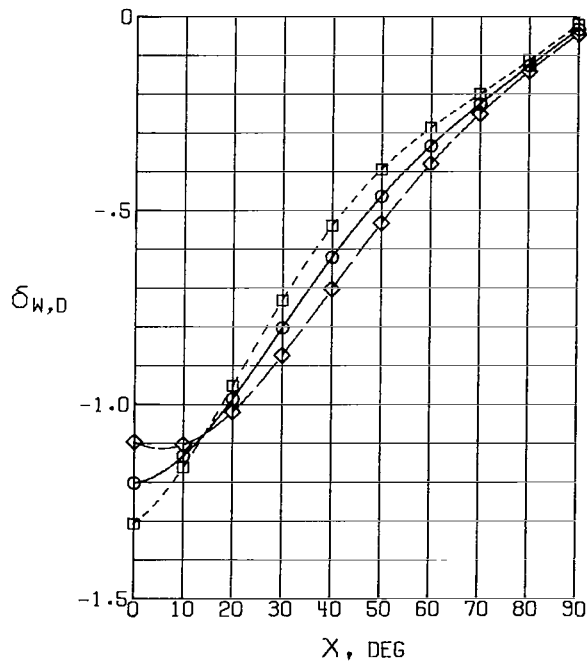
Figure 2.- Concluded.



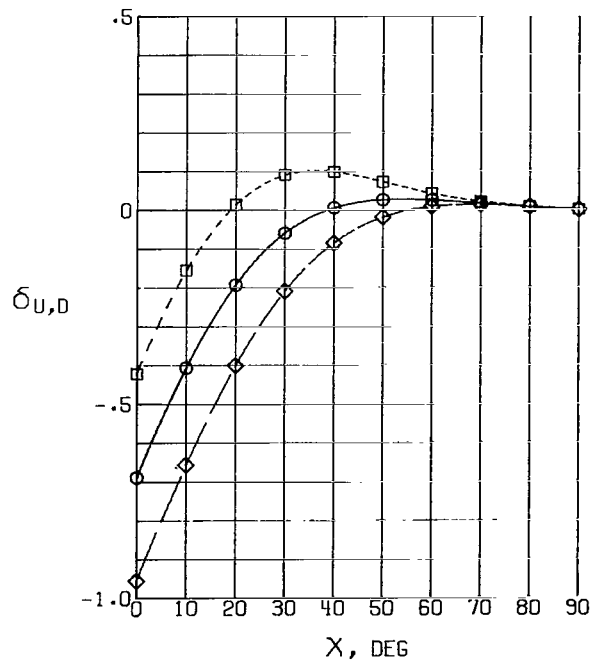
(a) Vertical interference due to lift.



(b) Horizontal interference due to lift.



(c) Vertical interference due to drag.



(d) Horizontal interference due to drag.

Figure 3.- Interference factors at model centered in tunnel.

Symbols show the shape of test section.

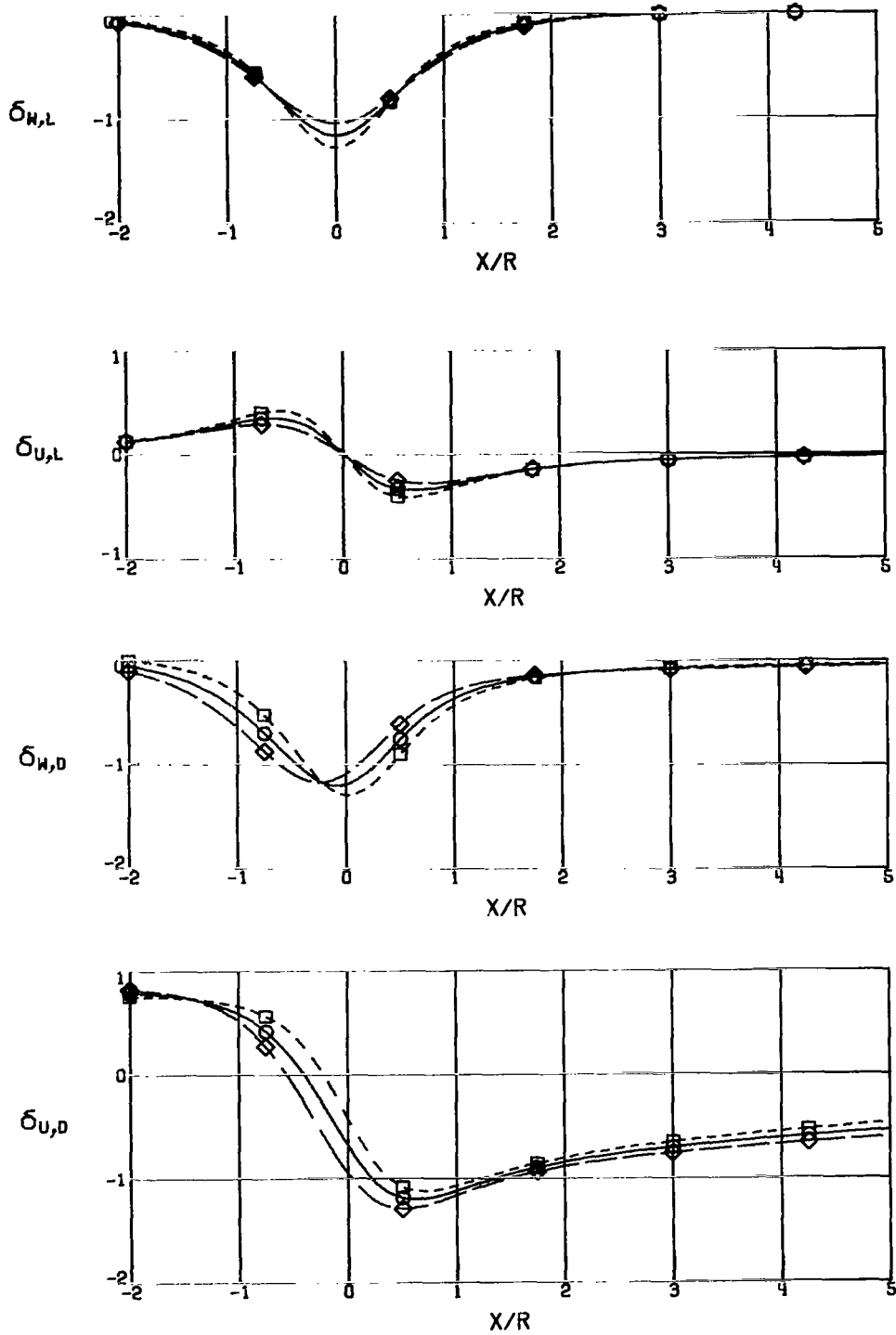


Figure 4.- Distribution of interference factors over longitudinal axis of tunnel. Shape of symbol denotes shape of test section. $\chi = 0^\circ$.

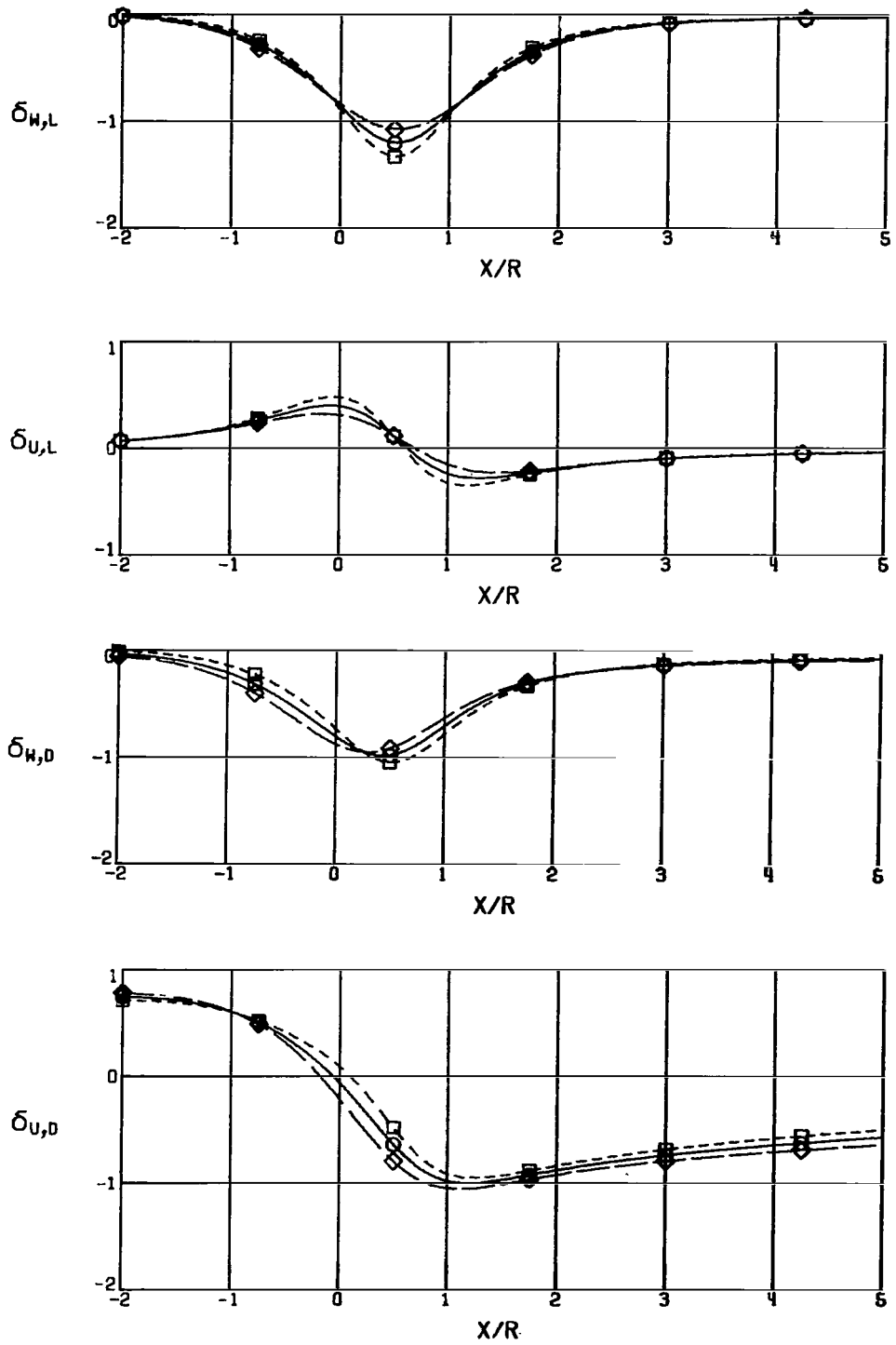


Figure 5.- Distribution of interference factors over longitudinal axis of tunnel. Shape of symbols denotes shape of test section. $\chi = 30^\circ$.

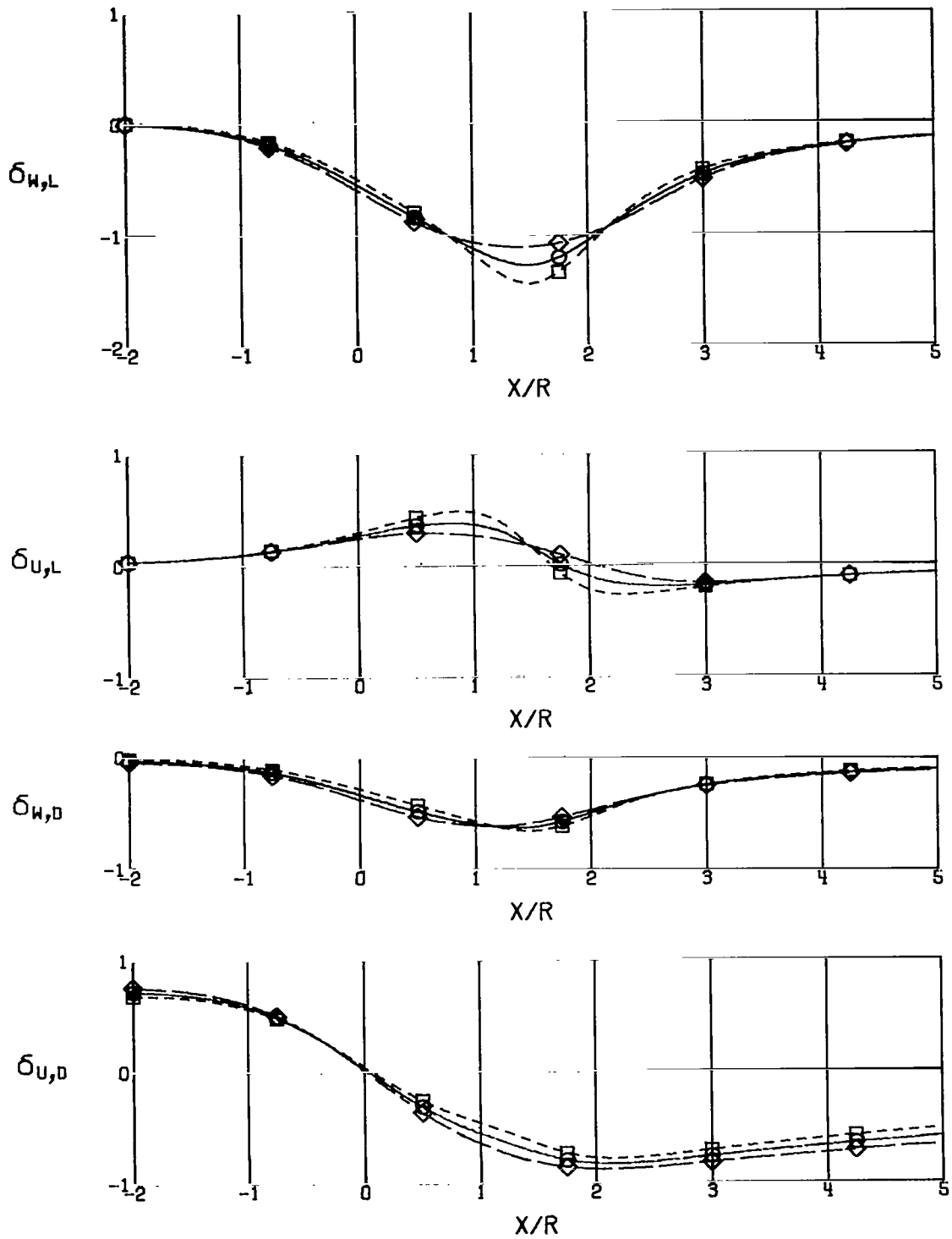


Figure 6.- Distribution of interference factors over longitudinal axis of tunnel. Shape of symbols denotes shape of test section. $\chi = 60^\circ$.

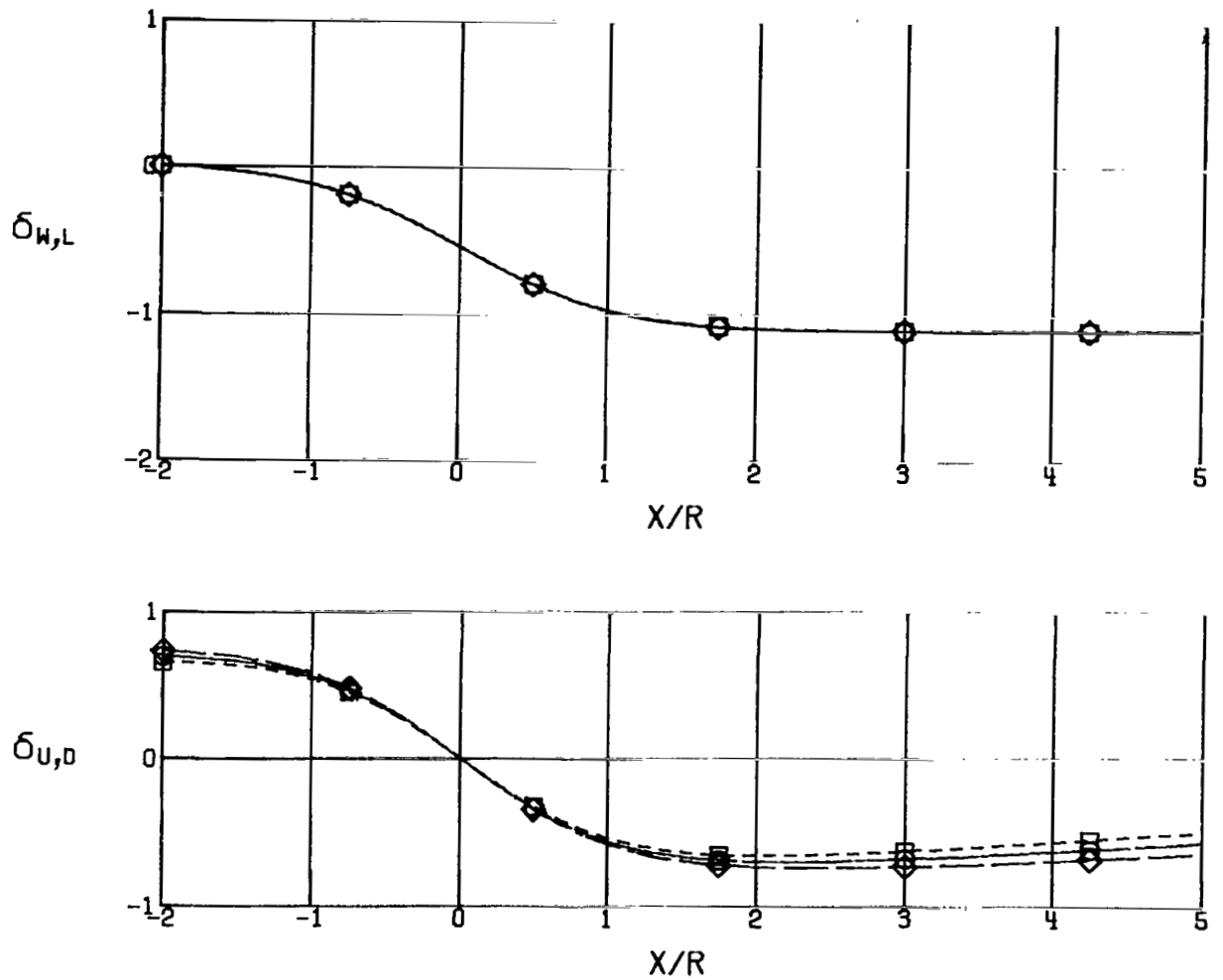


Figure 7.- Distribution of interference along longitudinal axis of tunnel. Shape of symbols denotes shape of test section. $\chi = 90^\circ$. (Note that for this skew angle, symmetry demands that $\delta_{u,L} = \delta_{w,D} = 0$.)

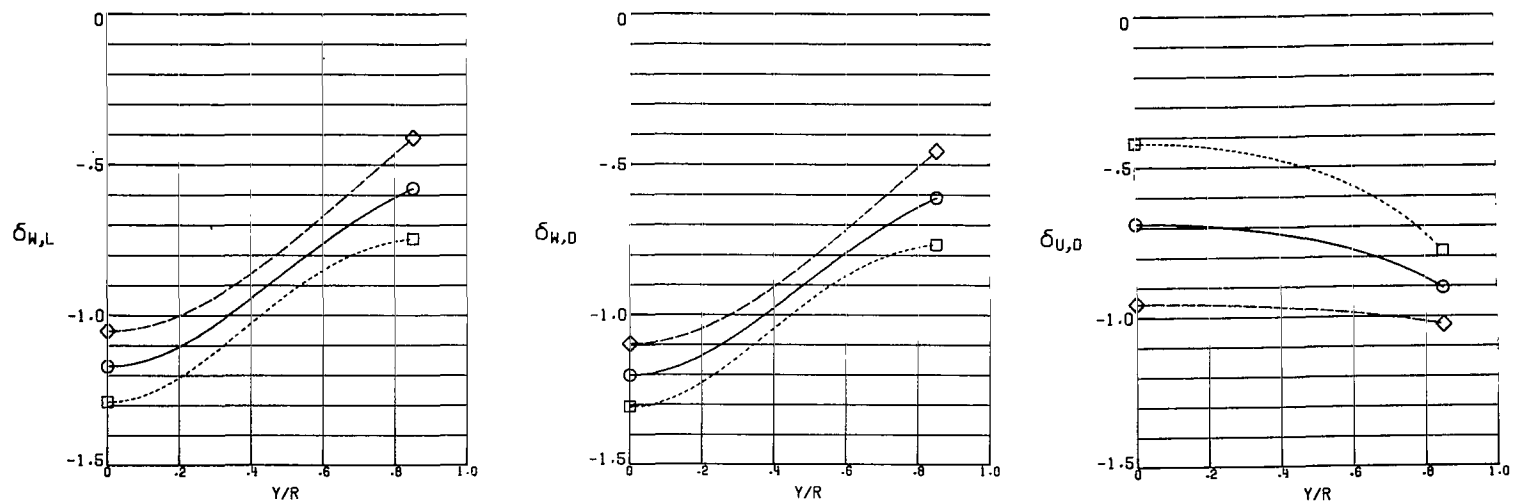


Figure 8.- Distribution of interference factors over lateral axis of tunnel. Shape of symbols denotes shape of test section. $\chi = 0^{\circ}$. (Note that for this skew angle, $\delta_{u,L} = 0$.)

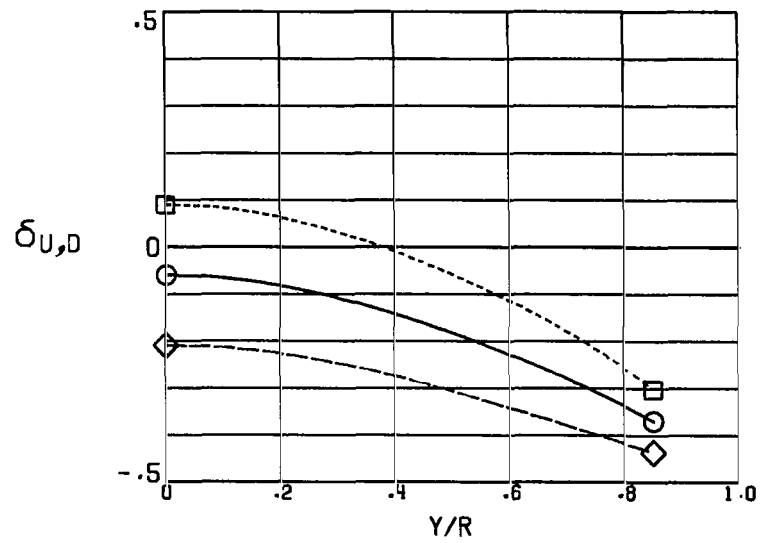
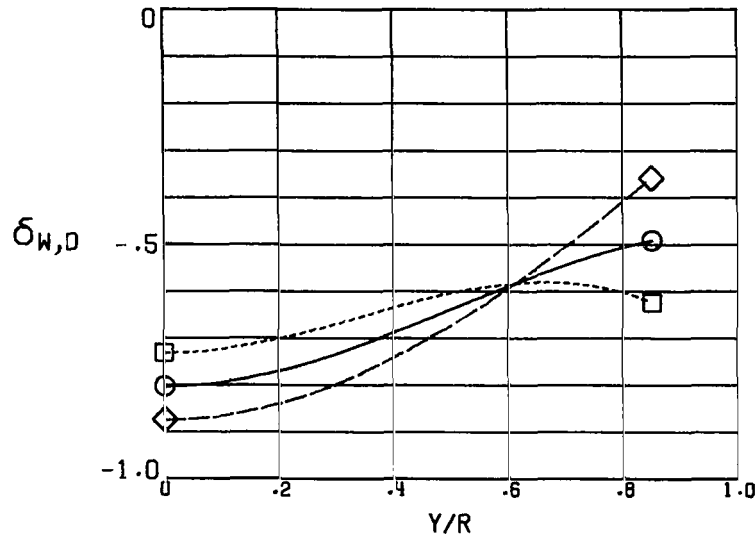
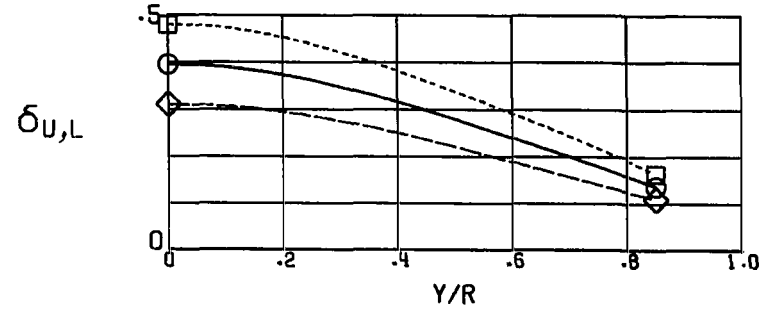
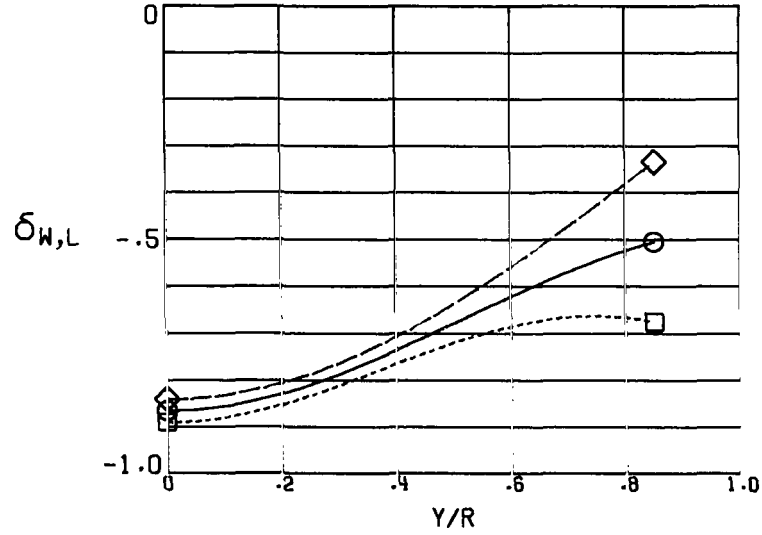


Figure 9.- Distribution of interference factors over lateral axis of tunnel. Shape of symbols denotes shape of test section. $\chi = 30^\circ$.

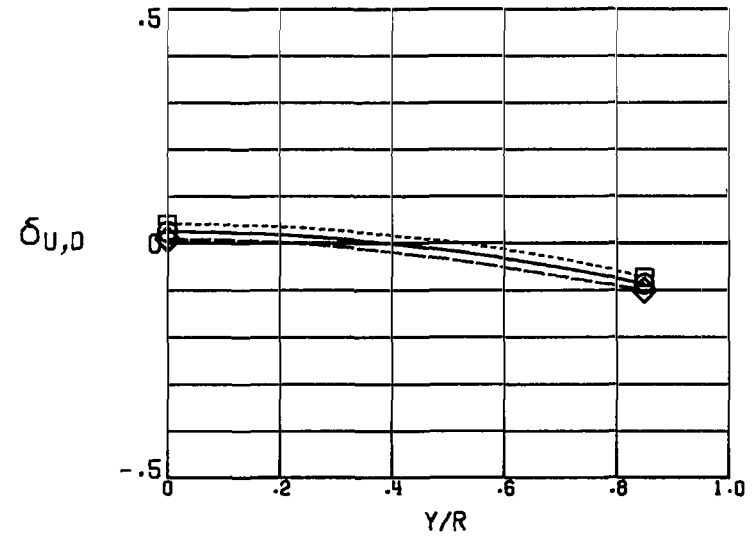
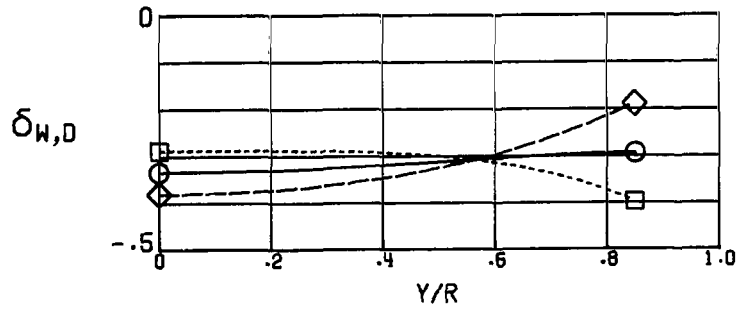
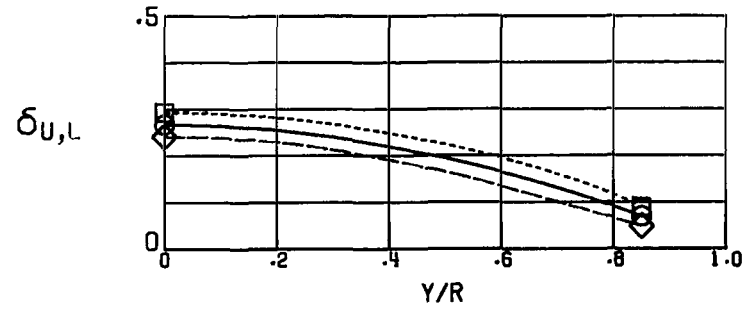
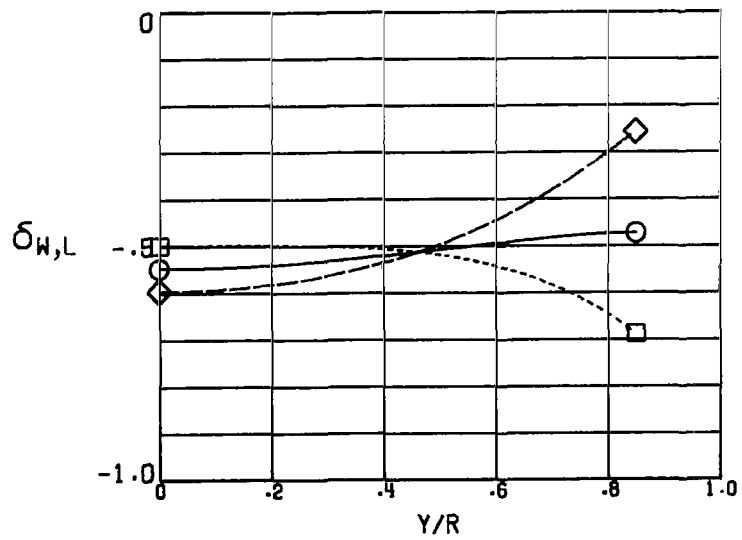


Figure 10.- Distribution of interference factors over lateral axis of tunnel. Shape of symbols denotes shape of test section. $\chi = 60^\circ$.

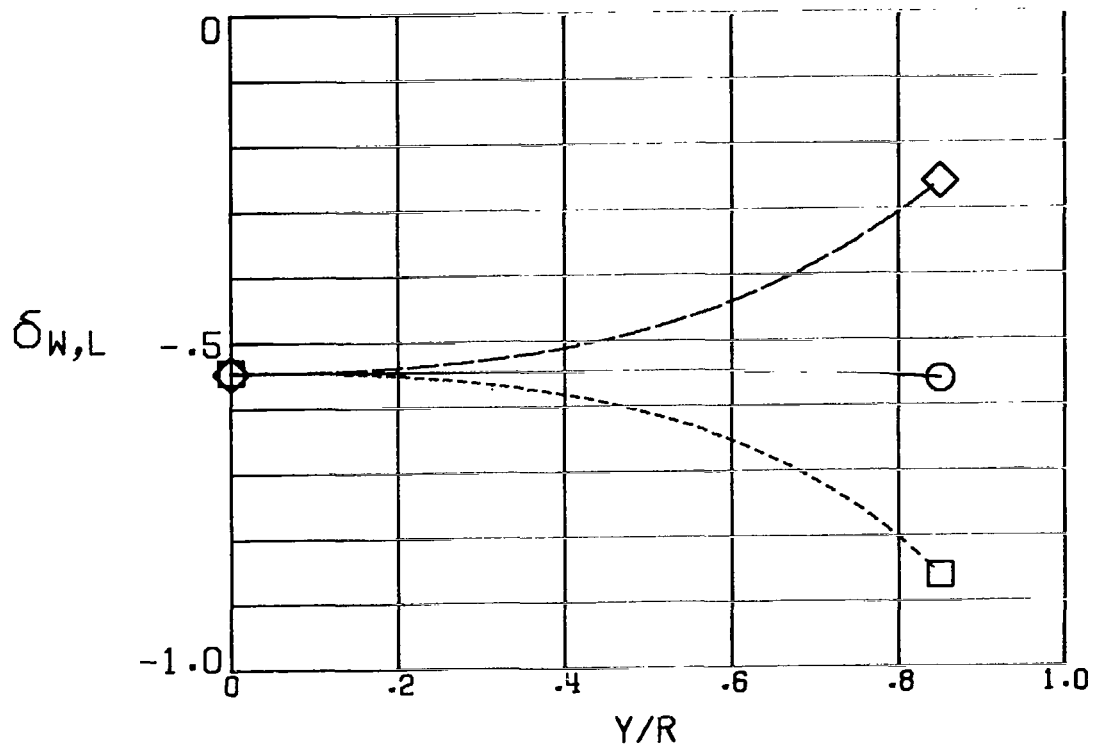


Figure 11.- Distribution of interference factors along lateral axis of tunnel. Shape of symbols denotes shape of test section. $\chi = 90^\circ$. (At $\chi = 90^\circ$, $\delta_{u,L}$, $\delta_{w,D}$, and $\delta_{u,D}$ are all zero over the entire axis.)

FIRST CLASS MAIL



POSTAGE AND FEES PA
NATIONAL AERONAUTICS
SPACE ADMINISTRATIC

02U 001 26 51 3DS 71028 00903
AIR FORCE WEAPONS LABORATORY /WLOL/
KIRTLAND AFB, NEW MEXICO 87117

ATT E. LOU BOWMAN, CHIEF, TECH. LIBRARY

POSTMASTER: If Undeliverable (Section
Postal Manual) Do Not R.

"The aeronautical and space activities of the United States shall be conducted so as to contribute . . . to the expansion of human knowledge of phenomena in the atmosphere and space. The Administration shall provide for the widest practicable and appropriate dissemination of information concerning its activities and the results thereof."

— NATIONAL AERONAUTICS AND SPACE ACT OF 1958

NASA SCIENTIFIC AND TECHNICAL PUBLICATIONS

TECHNICAL REPORTS: Scientific and technical information considered important, complete, and a lasting contribution to existing knowledge.

TECHNICAL NOTES: Information less broad in scope but nevertheless of importance as a contribution to existing knowledge.

TECHNICAL MEMORANDUMS: Information receiving limited distribution because of preliminary data, security classification, or other reasons.

CONTRACTOR REPORTS: Scientific and technical information generated under a NASA contract or grant and considered an important contribution to existing knowledge.

TECHNICAL TRANSLATIONS: Information published in a foreign language considered to merit NASA distribution in English.

SPECIAL PUBLICATIONS: Information derived from or of value to NASA activities. Publications include conference proceedings, monographs, data compilations, handbooks, sourcebooks, and special bibliographies.

TECHNOLOGY UTILIZATION PUBLICATIONS: Information on technology used by NASA that may be of particular interest in commercial and other non-aerospace applications. Publications include Tech Briefs, Technology Utilization Reports and Technology Surveys.

Details on the availability of these publications may be obtained from:

SCIENTIFIC AND TECHNICAL INFORMATION OFFICE

NATIONAL AERONAUTICS AND SPACE ADMINISTRATION

Washington, D.C. 20546